Strain Rate Effects on Tensile Deformation of 2024-O and 7075-O Aluminum Alloy Sheet

R.C. Dorward and K.R. Hasse

Coarse- and fine-grained 2024 and 7075 alloy sheets were tensile tested at strain rates ranging from 10^{-3} to 10^{2}/s. Ultimate tensile strengths decreased up to 10^{-1}/s and increased at higher strain rates. Total elongations at failure showed the same behavior with uniform and localized components showing similar dependencies on strain rate. The initial ductility decrease at low strain rates is attributed to thermal gradients associated with a transition from isothermal to adiabatic conditions. At strain rates above 10^{-1}/s, ductility increases as strain rate hardening effects become dominant. Although the fine-grained materials had higher elongations than their coarse-grained counterparts, both variants responded similarly to changes in strain rate. The only difference was a tendency for off-center failures in coarse-grained specimens tested at the slower strain rates.

Keywords
aluminum alloys, 2024 alloy, 7075 alloy, strain rate, sheets

1. Introduction

THE TENSILE and compressive flow stresses of aluminum alloys are known to be relatively independent of strain rate below 10^{3}/s. For example, compression tests on O temper (fully annealed) 2024 and 7075 alloys have shown slight increases in flow stress above strain rates of about 0.5/s (Ref 1). Based on these published data and the common constitutive equation

$$\sigma = \sigma_0 \varepsilon^n \dot{\varepsilon}^m (1 - \beta \Delta T)$$

the strain rate sensitivity index m is estimated to be in the 0.007 to 0.010 range (σ is the flow stress, ε is strain, n is the work hardening coefficient, $\dot{\varepsilon}$ is strain rate, T is temperature, and σ_0 and β are constants). According to Higashi et al. (Ref 2), some alloys appear to exhibit a decrease in tensile flow stress in the 10^{-2} to 10^{2}/s range, with significant increases at strain rates above 10^{3}/s. Other results (Ref 3) show a modest increase in flow stress over the 10^{-4} to 10^{3}/s range, the effect being inversely dependent on yield strength.

Of more interest from a formability viewpoint is the dependence of tensile elongation on strain rate. In principle, the uniform elongation should be independent of strain rate under isothermal (or adiabatic) conditions unless n or m are strain rate dependent. Measured elongations in a number of aluminum alloys increase with strain rate (Ref 2), with the greatest effect occurring above about 10^{3}/s, although Al-Mg alloy 5454 showed significant effects in the 10^{1} to 10^{3}/s range (Ref 3). The latter study attributed the increase in elongation almost entirely to deformation after the onset of necking, but other work indicates that the relative contributions of uniform and localized (necking) components are somewhat uncertain (Ref 4).

R.C. Dorward and **K.R. Hasse**, Center for Technology, Kaiser Aluminum & Chemical Corporation, Pleasanton, CA 94566, USA.

Studies on other materials, however, have shown a decrease in elongation with increasing strain rate (Ref 5-7), whereby plastic adiabaticity results in thermal gradients, in which strain and strain-rate hardening compete with thermal softening. These thermal effects appear particularly operative in the post-uniform deformation regime (Ref 7-8), i.e., the stabilizing influence of rate sensitivity is mitigated by temperature gradients in the diffuse neck region. Finally, at strain rates above about 10^{3}/s, inertial factors become significant (Ref 9-11), which generally have a strong positive effect on ductility. Within a certain range of "dynamic" strain rates (10^{1} to 10^{2}/s), a ductility minimum may be expected (Ref 10).

Although the tensile properties of a number of aluminum alloys have been examined as a function of strain rate (Ref 2-4, 9), no studies have been conducted on aircraft AA2024 and AA7075 sheet products, which are commonly formed in the annealed (O temper) condition and subsequently heat treated to the T4 and T6 tempers. We present here such data for these materials over the nominal strain rate range of 10^{-3} to 10^{2}/s. Since the alloys are supplied in relatively coarse-grained (batch annealed) and fine-grained (continuously annealed) structures, both conditions were evaluated.

2. Experimental

Tensile specimens with a 50-mm gage length and a 12.5-mm width (ASTM E8) were machined in the transverse direction from 1.6-mm-thick production sheets of the nominal compositions shown in Table 1.

A Universal Instron (Instron Corporatron, Canton, MA) testing machine was used for tests at cross head speeds of 2.5,

Table 1 Nominal compositions of 2024 and 7075 alloy sheets

Alloy	Composition, wt%							
	Si	Fe	Cu	Mn	Mg	Cr	Zn	Ti
2024	0.10	0.25	4.50	0.55	1.40	0.00	0.10	0.02
7075	0.10	0.25	1.45	0.10	2.50	0.20	5.65	0.02

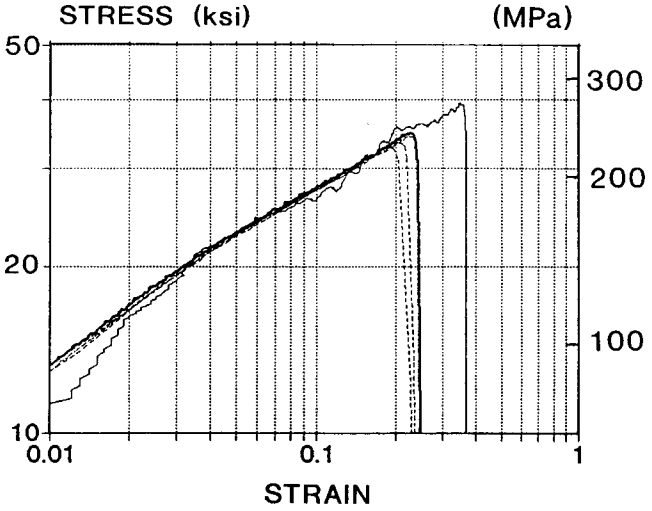

Fig. 1 True stress-true strain curves for coarse-grained 2024-O at strain rates from 8×10^{-4}/s (heavy line) to 80/s (light wavy line).

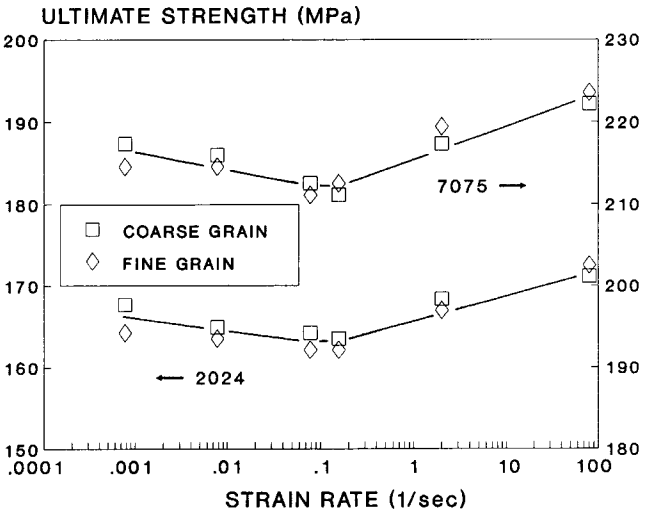

Fig. 2 Effect of strain rate on the ultimate tensile strength of 2024-O and 7075-O sheet.

25, 250, and 500 mm/min (initial strain rates of 8.33×10^{-4}, 8.33×10^{-3}, 8.33×10^{-2}, an 1.67×10^{-1}/s). Digital data acquisition was achieved using Instron DSA Series IX software (Instron Corporation Canton, MA). Displacements and elongations were obtained from an extensometer attached to the specimens. "Machine" elongations were also checked against manual measurements on the broken specimens. MTS Systems Corporation (Eden Prairie, MN) servohydraulic machines were used for the higher strain rate tests. At a ram speed of 6850 mm/min (2.25/s), a standard ??? (MTS) load cell and hydraulic grips were used, with light oscillograph recordings of analog load-displacement outputs. Tests at the highest strain rate (85/s) utilized special low-mass grips and a slack drawbar to minimize harmonic effects. The data were captured with a Nicolette digital storage scope (company). Displacements were obtained with internal linear variable differential transformers (LVDTs) on the MTS machines, but elongations were measured manually on the broken specimens. For another measure of ductility, reductions of area were determined 12.5 mm from the fractures. Similarly R values (ratio of thickness to width strains) were measured at this location. All tests were conducted in still air at ambient temperature (21 to 24 °C).

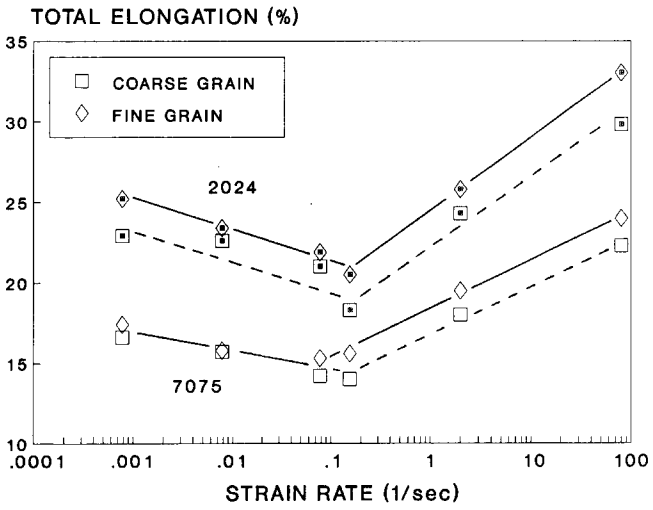

Fig. 3 Effect of strain rate on the total tensile elongation of 2024-O and 7075-O sheet.

3. Results

True stress-true strain curves covering the complete range of strain rates are shown in Fig. 1. There appeared to be little effect of strain rate on the stress-strain behavior in the low stress region. Ultimate stresses and elongations at maximum load and at failure, however, did depend on strain rate. Figure 2 shows that the ultimate strength decreased up to about 0.1/s and then increased at higher strain rates, with no apparent influence of grain structure in either alloy. Yield strengths (0.2% proof stress) showed the reverse trend, increasing 15 to 20% up to 0.2/s. We were unable to make accurate assessments of yield strength at the higher strain rates because of noise in the data acquisition systems. As would be expected from the similarity of the stress-strain curves, work hardening rates were not significantly affected by strain rate over the 10^{-3} to 10^{-1}/s range. For 2024, average n values were 0.207 (fine grain) and 0.204 (coarse grain); the corresponding values for 7075 were 0.176 and 0.164.

The effect of strain rate on total elongation is shown in Fig. 3. As with ultimate strength, elongation decreased up to about 0.2/s and then increased fairly dramatically. Note that these ductility variations are not related to differences in data retrieval systems. Elongations at the two highest strain rates were measured manually, and values at the low strain rates were checked identically. Elongations in fine-grained 2024 alloy were consistently higher than those in the coarse-grained materials, which was expected (Ref 12). The fine-grained version of 7075 was also more ductile at the higher strain rates. On a nor-

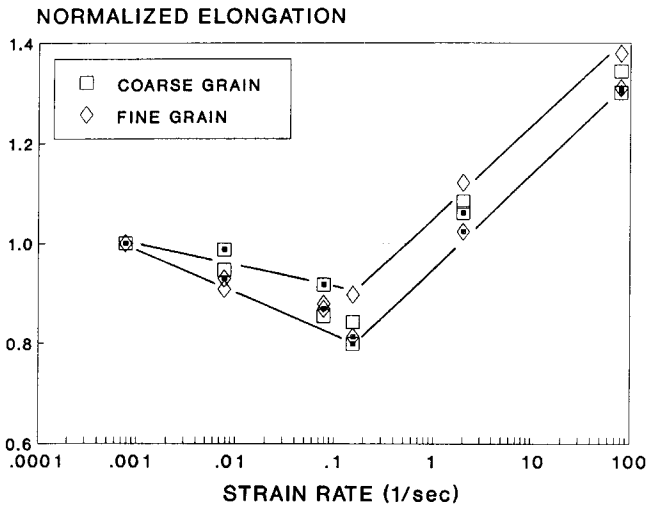

Fig. 4 Normalized elongation vs. strain rate for 2024-O and 7075-O sheet.

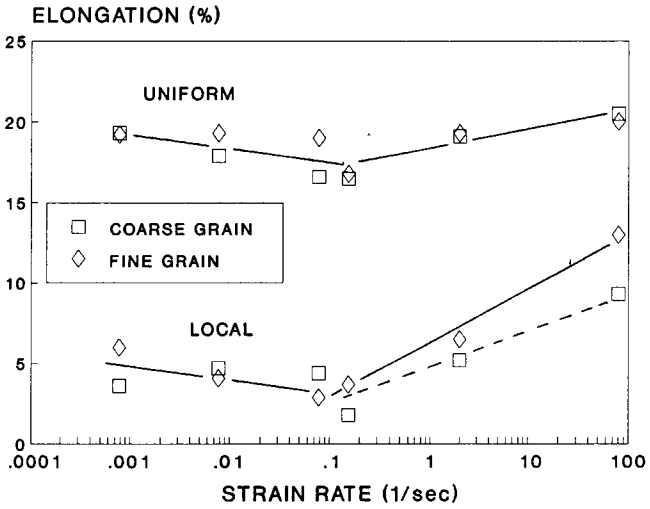

Fig. 5 Effect of strain rate on the uniform and local (postuniform) elongation of 2024-O sheet.

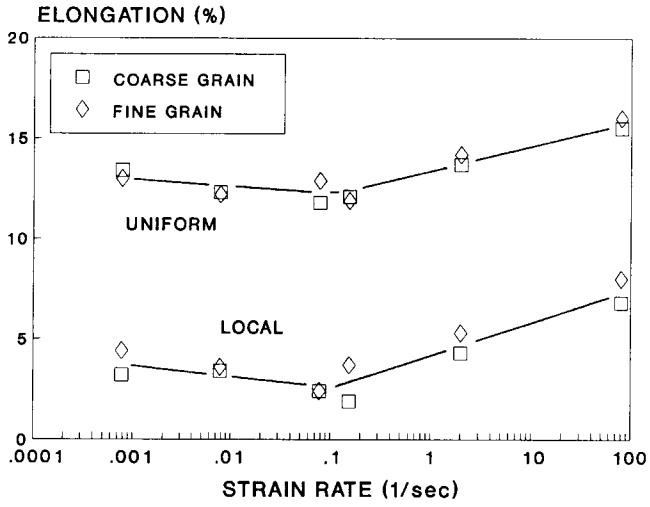

Fig. 6 Effect of strain rate on the uniform and local (postuniform) elongation of 7075-O sheet.

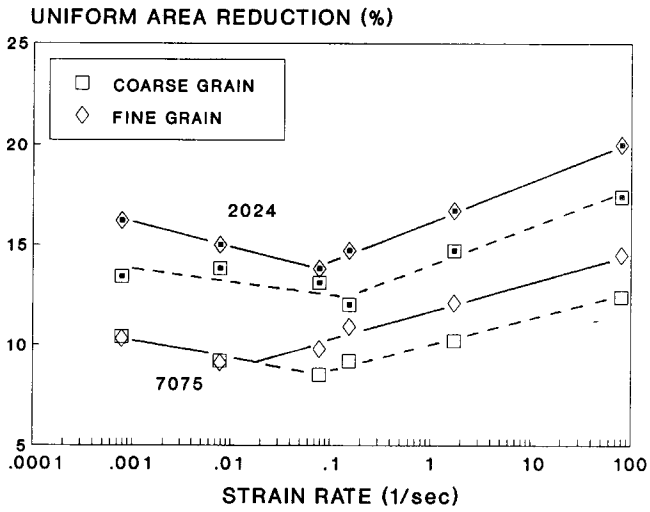

Fig. 7 Effect of strain rate on the uniform reduction of area of 2024-O and 7075-O sheet.

malized basis, both alloys showed essentially identical behavior within experimental error (Fig. 4).

Total elongations were divided into their uniform (displacement at maximum load) and localized components (by difference) and plotted against strain rate as shown in Fig. 5 and 6. Both ductility indicators showed similar behavior, with localized elongation appearing somewhat more dependent at high strain rates. Figure 7 shows that uniform area reduction, as measured 12.5 mm from the fractures, had the same behavior as uniform elongation based on displacement at maximum load, even though the absolute values were somewhat lower. Although difficult to quantify on a flat tensile specimen, it was visually obvious that reductions of area at the fracture face were also significantly greater in specimens tested at the higher strain rates. Elongation and reduction of area measurements, therefore, support the contention that both uniform and localized deformation are enhanced at strain rates in the 10^{-1} to 10^{2}/s range.

Fractures in the fine-grained materials generally occurred within 5 mm of the specimen center. However, at the slow strain rates, failures in the coarse-grained sheets were located on average 10 to 15 mm from the specimen center (Fig. 8). At strain rates above 10^{-1}/s there were no significant differences in failure position between the coarse and fine-grained materials.

Within experimental detection limits based on specimen width and thickness measurements, there was little effect of strain rate on thickness-to-width strain ratios (R values). The only material that appeared to mirror the elongation behavior was the coarse-grained 7075 sheet (Fig. 9). Interestingly, the coarse-grained 7075 material also had consistently higher R values than its fine-grained counterpart, whereas 2024 showed the opposite response: the coarse-grained variant had consistently lower R values (and lower total elongations).

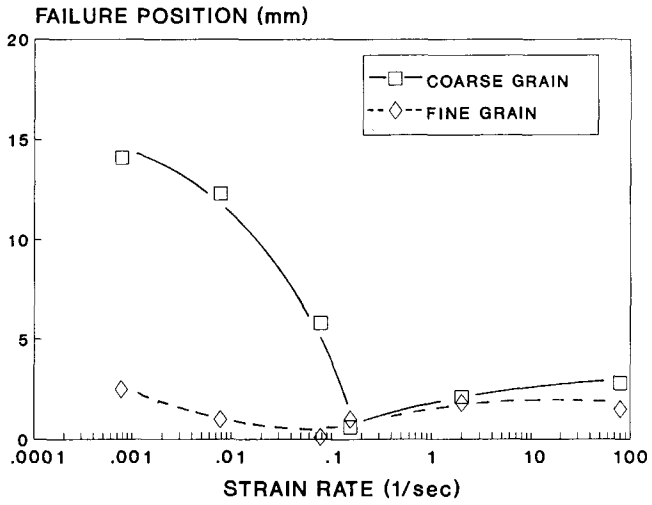

Fig. 8 Average failure position (distance from center) vs. strain rate for both alloys.

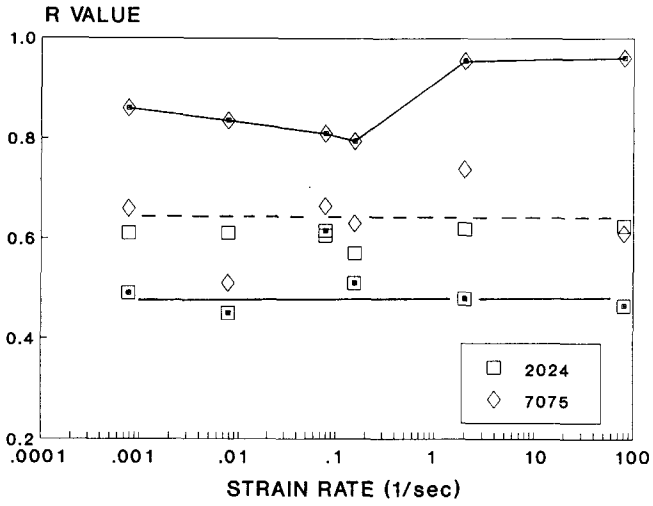

Fig. 9 *R* values of coarse-grained (closed symbols, solid lines) and fine-grained (open symbols, dashed line) O temper sheet.

4. Discussion

A number of experimental findings warrant further attention and examination.

Tensile stress-strain curves in the yield-to-ultimate range were relatively unaffected by strain rates of 10^{-3} to 10^{2}/s. This implies little effect of strain rate on work hardening rate (*n* values).

Ultimate strengths decreased slightly in the 10^{-3} to 10^{-1}/s range and then increased moderately above 10^{-1}/s. Yield strengths increased somewhat in the 10^{-2} to 10^{-1}/s range. Ultimate strengths correlated with elongation as discussed below.

Total elongation to failure decreased up to 10^{-1}/s, and on a normalized basis all materials behaved in the same manner. Both uniform and localized elongation decreased slightly in the 10^{-3} to 10^{-1}/s range. Reduced elongation in this range is probably related to the transition from isothermal to adiabatic conditions, i.e., the development of thermal gradients. According to theoretical calculations and experimental measurements, adiabatic conditions (minimum ductility) for tests in air should be achieved at strain rates of 10^{-2} to 10^{-1}/s (Ref 5, 13). Although claims have been made that postuniform elongation should be affected most by such thermal gradients (Ref 8), reductions in both uniform and local elongations have been observed (Ref 5, 6).

At strain rates above 10^{-1}/s, total elongation increased rapidly; and again, both uniform and localized ductility were affected, although the latter appeared more dependent. Increased elongation in the 10^{-1} to 10^{2}/s range cannot be ascribed to inertia because such effects do not become apparent until strain rates exceed about 10^{3}/s (Ref 10, 11). Instead, it seems more likely that strain rate sensitivity plays an important role; i.e., the negative effects of thermal gradients are more than offset by an increase in *m*. And, as noted by Ghosh (Ref 14), postuniform deformation should be affected most. The modest rise in uniform elongation (and reduction of area) in this strain rate range suggests an increase in work hardening rate (*n*). Although such an effect was not apparent in the slope of the stress-strain curves, the translation of the load-deflection curves is not strictly accurate because of the thermal and deformation gradients (Ref 6).

At low strain rates, tensile specimens from coarse-grained materials failed off-center. Ferron (Ref 6) has shown that under near-isothermal conditions, failures in type 304 stainless steel tend to occur randomly over the specimen length, but show a preferential location near the center when the test conditions favor higher temperatures in this region. Presumably, the larger grains are effective initiators of inhomogeneous strain, which eventually develop into "active" necks. As the strain rate increases, larger temperature gradients lead to an earlier promotion of such defects located near the center. The fine-grained materials, on the other hand, neck "normally" in the slightly reduced cross section at the specimen center.

5. Summary

The deformation of 2024-O and 7075-O tensile specimens is a complex process involving the competing effects of a number of physical phenomena: strain and strain rate hardening, and strain-rate dependent thermal gradients and softening. Decreasing ductility with increasing strain rate in the low strain rate regime is attributed to a transition from isothermal to adiabatic conditions. At higher strain rates, strain rate hardening effects dominate, and ductility increases.

Acknowledgement

We wish to thank W. Kawahara, J. Korellis and J. Totten of Sandia National Laboratory (Livermore) for conducting the 85/s strain rate tests.

References

1. D.L. Holt, S.G. Babcock, S.J. Green, and C.J. Maiden, The Strain-Rate Dependence of the Flow Stress in Some Aluminum Alloys, *Trans. ASM*, Vol 60, 1967, p 152-158

2. K. Higashi, T. Mukai, K. Kaizu, S. Tsuchida, and S. Tanimura, Strain Rate Dependence on Mechanical Properties in Some Commercial Aluminum Alloys, *J. Phys. IV*, Vol 1, 1991, p C3/341-346
3. U.S. Lindholm, R.L. Bessey, and G.V. Smith, Effect of Strain Rate on Yield Strength, Tensile Strength, and Elongation of Three Aluminum Alloys, *J. Mater*, Vol 6, 1971, p 119-131
4. T. Mukai, K. Higashi, S. Tsuchida, and S. Tanimura, Influence of Strain Rate on Tensile Properties in Some Commercial Aluminum Alloys, *J. Jpn. Inst. Light Met.*, Vol 43, 1993, p 252-257
5. A.S. Korhonen and H.J. Kleemola, Effects of Strain Rate and Deformation Heating in Tensile Testing, *Metall. Trans. A*, Vol 9, 1978, p 979-985
6. G. Ferron, Influence of Heat Generation and Conduction on Plastic Stability under Uniaxial Tension, *Mater Sci. Eng.*, Vol 49, 1981, p 241-248
7. R.A. Ayres, Thermal Gradients, Strain Rate, and Ductility in Sheet Steel Tensile Specimens, *Metall. Trans. A*, Vol 16 ,1985, p 37-43
8. S.I. Semiatin, R.A. Ayres, and J.J. Jonas, An Analysis of the Non-isothermal Tensile Test, *Metall. Trans. A*, Vol 16 , 1985, p 2299-2308
9. R.N. Orava, The Effect of Dynamic Strain Rates on Room Temperature Ductility, *1st Int. Conf. on High Energy Forming*, 1967, U.S. Dept. of Commerce Rept., p 87-116
10. C. Fressengeas and A. Molinari, Inertia and Thermal Effects on the Localization of Plastic Flow, *Acta Metall.*, Vol 33, 1985, p 387-396
11. G. Regazzoni, J.N. Johnson, and P.S. Follansbee, Theoretical Study of the Dynamic Tensile Test, *J. Appl. Mech.*, Vol 53, 1986, p 519-528
12. R.C. Dorward, Forming Characteristics of Coarse and Fine-Grained AA2024 Aluminum Alloy Sheet, *J. Mater Eng. Perform.*, Vol 3, 1994, p 115-121
13. Y. Gao and R.H. Wagoner, A Simplified Model of Heat Generation during the Uniaxial Tensile Test, *Metall. Trans. A*, Vol 18, 1987, p 1001-1009
14. A.K. Ghosh, A Numerical Analysis of the Tensile Test for Sheet Metals, *Metall. Trans. A*, Vol 8 ,1977, p 1221-1232